PHYSICAL REVIEW B **89**, 081408(R) (2014)

Valence bond liquid phase in the honeycomb lattice material Li_2RuO_3

Simon A. J. Kimber,[1,*] I. I. Mazin,[2] Juan Shen,[3] Harald O. Jeschke,[3] Sergey V. Streltsov,[4,5] Dimitri N. Argyriou,[6,7] Roser Valentí,[3,†] and Daniel I. Khomskii[8]

[1]*European Synchrotron Radiation Facility (ESRF), 6 rue Jules Horowitz, BP 220, 38043 Grenoble Cedex 9, France*
[2]*Code 6393, Naval Research Laboratory, Washington, DC 20375, USA*
[3]*Institut für Theoretische Physik, Goethe-Universität Frankfurt, 60438 Frankfurt am Main, Germany*
[4]*Institute of Metal Physics, S. Kovalevskaya Street 18, 620041 Ekaterinburg, Russia*
[5]*Ural Federal University, Mira Street 19, 620002 Ekaterinburg, Russia*
[6]*European Spallation Source ESS AB, Box 176, 22100 Lund, Sweden*
[7]*Department of Synchrotron Research, Lund University, Box 118, Lund, Sweden*
[8]*II. Physikalisches Institut, Universität zu Köln, Zülpicher Strasse 77, 50937 Köln, Germany*

(Received 29 October 2013; revised manuscript received 15 January 2014; published 27 February 2014)

The honeycomb lattice material Li_2RuO_3 undergoes a dimerization of Ru^{4+} cations on cooling below 270 °C, where the magnetic susceptibility vanishes. We use density functional theory calculations to show that this reflects the formation of a valence bond crystal, with a strong structural bond disproportionation. On warming, x-ray diffraction shows that discrete threefold symmetry is regained on average, and the dimerization apparently disappears. In contrast, local structural measurements using high-energy x rays show that disordered dimers survive at the nanoscale up to at least 650 °C. The high-temperature phase of Li_2RuO_3 is thus an example of a valence bond liquid, where thermal fluctuations drive resonance between different dimer coverages, a classic analog of the resonating valence bond state often discussed in connection with high-T_c cuprates.

DOI: 10.1103/PhysRevB.89.081408 PACS number(s): 61.05.cp, 61.05.fm, 61.50.−f, 71.15.Mb

Introduction. Honeycomb layered systems are of particular interest in solid state physics, due to their fascinating electronic, magnetic, and superconducting properties. Recently, honeycomb iridates A_2IrO_3 (A=Li, Na) have attracted a lot of attention due to the presence of large spin-orbit coupling that was suggested to lead to interesting topological properties [1] and possibly to unconventional Kitaev magnetic interactions [2]. The latter proposition, however, is presently under discussion [3]. Analogs containing 4*d* metals, where the spin-orbit coupling is much weaker, might thus offer further insights into the iridates [4].

A well known member of the 4*d* family is Li_2RuO_3, which is similar to Li_2RhO_3 and Na_2IrO_3, but with one more hole in the transition-metal t_{2g} bands. In Li_2RuO_3 an intriguing ground state is found below ∼270 °C, where the Ru atoms form structural dimers with a very strong disproportionation of the short and long bonds ($l_l/l_s \sim 1.2$) [5]. The origin of this dimerization is controversial, and it has been unclear to what extent this behavior is present in the corresponding d^5 compounds; existing experimental evidence suggests that Na_2IrO_3 remains highly symmetric, with less than a 3% variation in Ir-Ir distances [3], and the same is probably true for Li_2RhO_3 and Li_2IrO_3 [4,6]. On the other hand, the relatively low quality of Li_2RhO_3 [4] and Li_2IrO_3 [6] samples does not allow excluding a possible local structural dimerization without long-range order, in which case the average crystal structure remains symmetric, but the electronic physics would be strongly influenced by a local-scale dimerization. To assess this possibility, we investigate here the microscopic origin of the well established dimerization in Li_2RuO_3 by a combination of x-ray diffraction, high-energy x-ray measurements, and density functional theory (DFT) calculations.

In this Rapid Communication, (i) we show that the tendency to dimerization in Li_2RuO_3 is local and driven by covalency as had been previously conjectured [5]. At low temperatures the local dimers show structural long-range order and form a valence bond crystal. (ii) We find experimentally that the dimerization locally survives well above the transition temperature ∼270 °C, forming a valence bond liquid (VBL). Approximately 1/3 of all Ru-Ru bonds are dimerized at all temperatures and the dimer ordering is short ranged with a correlation length of the order of a few nanometers at high temperatures. The VBL we propose is not to be confused with the so-called *resonating* valence bond (RVB) liquid [8] that has received much attention in connection with high-T_c cuprates; in the latter the many-body electron wave function is a linear combination of the electronic states with all possible spin singlets (called "valence bonds"). In particular one can define a RVB state with dimer singlets (short-range RVB) [9] where the *resonating* nature is a result of the quantum fluctuations. In the present case the valence bond liquid originates from existing dimer patterns that *resonate* due to thermal fluctuations and could be described as the classical analog of short-range RVB. (iii) Both the formation of local dimers with long-range order at low temperatures and the presence of a VBL above the transition temperature are supported by our DFT results. In our calculations, we find that the experimentally observed long-range order of Ru-Ru dimers at temperatures below 270 °C indeed gives the state with the lowest energy. However, other mutual arrangements of Ru-Ru dimers have similar energies, varying by ∼40 meV, and all dimerized patterns have the energy much lower (by ∼155 meV) than the energy of the uniform state. These results explain the fact that the long-range ordering of dimers is destroyed at $T_c \sim 270$ °C (∼47 meV), whereas dimers survive up to

*Corresponding author: kimber@esrf.fr
†Corresponding author: valenti@itp.uni-frankfurt.de

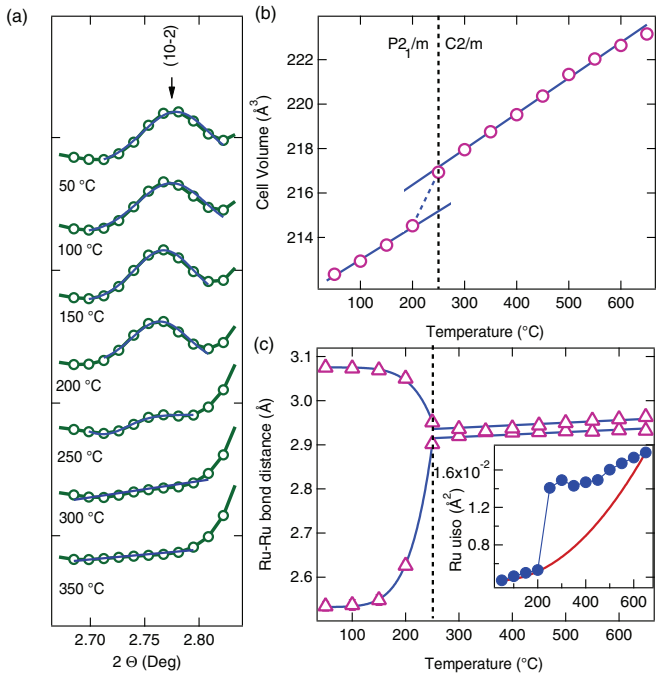

FIG. 1. (Color online) (a) Selected region of the x-ray diffraction profile of Li_2RuO_3 as a function of temperature, showing the disappearance of the (10-2) reflection at the structural phase transition. The tail to higher angles originates from the intense (11-2) reflection. (b) Temperature dependence of the refined unit cell volume of Li_2RuO_3. (c) Temperature dependence of the Ru-Ru bond distance extracted from Rietveld refinement against the powder x-ray diffraction data; the inset shows the refined Ru atomic displacement parameter with an extrapolated Debye dependence (red line).

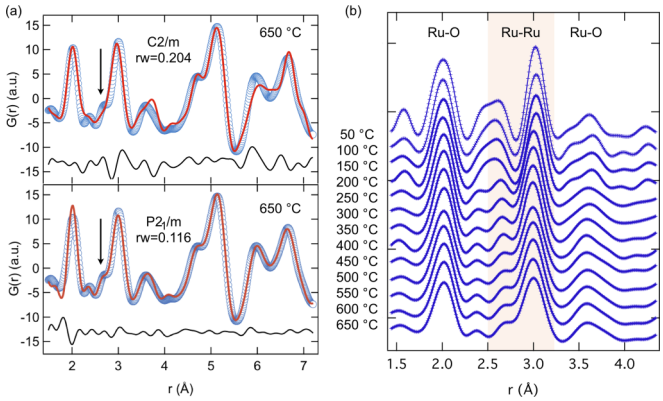

FIG. 2. (Color online) (a) Results of fitting the $C\,2/m$ (top) and $P\,2_1/m$ (bottom) structures via $G(r)$ to the PDF data at 650 °C (open blue circles: experiment; solid red lines: model calculations). The measured profile versus the calculated profile is the offset black line. (b) Temperature evolution of the PDF. The region containing the Ru-Ru bonds is highlighted and other important distances are also indicated.

much higher temperatures (VBL phase) and are consistent with our experimental observation that upon quenching the high-temperature phase to 50 °C the dimerization is recovered. The energy(∼155 meV) sets a temperature of ≈1500 °C for the disappearance of dimers which is reasonably consistent with our experimental estimate. Finally, by analyzing the total density of states (DOS), we conclude that not only the orbital identified in Ref. [7] contributes to the covalency of the dimerized bond via direct overlap, but also another orbital provides an additional contribution via an O-assisted hopping. These findings play a very important role in understanding the microscopic physics of other 4*d* and 5*d* honeycomb oxides as discussed above.

Experiment. We synthesized a ceramic sample of Li_2RuO_3, which was characterized by both neutron [10] and synchrotron x-ray powder diffraction. Both methods gave results consistent with the dimerized $P\,2_1/m$ structure reported in Ref. [5] at room temperature. Diffraction experiments were performed using the ID15B beamline at the ESRF, Grenoble. A wavelength of 0.1422 Å was used and the scattered x rays were detected by a Mar345 image plate. Two detector distances were used at each temperature, such that data suitable for both Rietveld [12] and pair distribution function analysis were collected (see Supplemental Material (SM) [11]). At room temperature, the dimerized structure is evidenced by the presence of $(h + k = \text{odd})$ reflections which break C centering [Fig. 1(a)]. The corresponding difference in Ru-Ru distances is pronounced, with 1/3 short bonds [13] (2.55 Å) and 2/3 long (∼3.1 Å) [see Fig. 4(a)]. Upon warming toward the transition, the $(h + k = \text{odd})$ reflections lose intensity, merging into the background above 250 °C. The refined Ru-Ru distances converge to a single value of ∼2.95 Å, and at 350 °C, excellent fits to the data were obtained using the undistorted $C\,2/m$ structure reported by Miura *et al.* [5] (see SM). The honeycomb layers are as symmetric as those seen [3,10] in the metallic honeycomb ruthenate $Ag_3LiRu_2O_6$ or Na_2IrO_3. Although the bond lengths converge in a manner indicative of a displacive phase transition [Fig. 1(c)], a small volume anomaly is also observed [Fig. 1(b)], with a slight expansion upon entering the high-temperature phase. Furthermore, a sharp increase in the Ru atomic displacement parameter is observed, which implies an increase in disorder beyond that expected in a simple Debye model [inset Fig. 1(c)].

Refinements against Bragg intensities are sensitive only to the average crystallographic structure. We therefore performed pair distribution function (PDF) analysis, which is sensitive to local order as it includes the diffuse scattering signal. Using Igor Pro based software (iPDF) developed by one of the authors (S.A.J.K.), we corrected the raw diffraction data for background, incoherent inelastic scattering, and the atomic form factors (see SM). To visualize any short-range disorder, we Fourier-transformed the structure factors $S(Q)$ defined in the reciprocal Q space into real space using $G(r) = \frac{2}{\pi}\int_0^\infty Q[S(Q) - 1]\sin(Qr)dQ$ where $G(r)$ describes the distribution of pairs of atoms separated by a distance r. Models were fitted to the PDF data using the PDFgui package [15].

Deep within the dimerized phase of Li_2RuO_3, we obtained good fits to the PDF data using the $P\,2_1/m$ crystal structure described above. However, upon examining the data at our highest temperature (650 °C), we found that the fit of the average $C\,2/m$ model was poor ($rw = 0.204$), when refined against the PDF data in the range $1.5 < r < 7.25$ Å [Fig. 2(a)]. In particular, the model does not reproduce a prominent peak (arrowed) at 2.68 Å. However, when we used the dimerized model which describes the low-temperature phase, this peak,

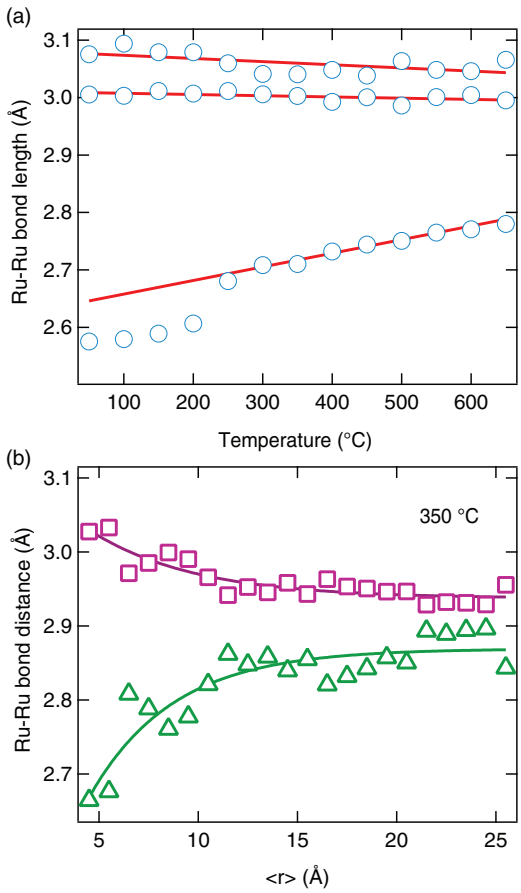

FIG. 3. (Color online) (a) Temperature dependence of the fitted Ru-Ru distances from the PDF analysis of Li_2RuO_3 in the range $1.5 < r < 7.25$ Å. Error bars obtained by directly fitting Gaussians to the data shown in Fig. 2(b) are smaller than the markers. (b) r dependence of the Ru-Ru distances extracted from model fits to the PDF at 350 °C as described in the text. The two inequivalent longer distances have been averaged for plotting.

and indeed the whole r range, was well fitted. The quality of the fit was nearly twice as good ($rw = 0.116$), and the 2.68 Å peak was due to Ru-Ru dimerization surviving at high temperatures. Furthermore, the excellent agreement of the $P\,2_1/m$ structure shows that l_l/l_s is approximately conserved. The PDF data at different temperatures are shown in Fig. 2(b). The peak corresponding to the short Ru-Ru distance is highlighted for the whole temperature region. Although there is a small shift of this peak to larger r values upon heating, the converging bond distances observed by Rietveld analysis [Fig. 1(c)] are clearly not observed on the local length scale. When we repeated refinements of the $P\,2_1/m$ structure on the local length scale for the whole temperature range, we obtained three equally populated Ru-Ru distances [14] which show an almost linear dependence on temperature [Fig. 3(a)] with only a small anomaly at the $P\,2_1/m \rightarrow C\,2/m$ transition. Extrapolating our data suggests that the short-range dimerization would persist up to at least $T_s \sim 1400$ °C, i.e., well beyond chemical decomposition. This energy scale T_s, which in a mean-field picture corresponds to the dimerization energy, is rather large for magnetic exchange interactions, although consistent with metal-metal covalent bonding [7,16] as we will show below. The energy scale of the ordering transition, ~47 meV, on the same level of approximation, should correspond to the interdimer interaction.

Having shown that the low-temperature $P\,2_1/m$ structure provides a reasonable model for the short-range dimer correlations at high temperatures, we then proceeded to investigate the length scale of this order. We performed so-called box-car refinement [17] of this structure against the PDF data at 350 °C. The so refined Ru-Ru distances are shown in Fig. 3(b). We find that the difference between the short and long bonds is progressively lost as the length scale increases demonstrating that the dimer order at $T = 350$ °C has a length scale of ~1.5 nm (about two unit cells). At even higher temperatures we found that the ordering of dimers vanishes beyond the first coordination sphere. Thus, at $T \gg T_c = 270$ °C there is little correlation between individual dimers, but ~1/3 of all Ru-Ru bonds remain dimerized.

Theory. The origin of the room-temperature dimerization has been discussed differently, depending on the starting point, i.e., localized versus itinerant description. Jackeli and Khomskii [18] considered a localized picture and argued that dimerization is controlled by orbital and spin physics, essentially, promoting singlet formation on the short bonds. A drastic reduction of the paramagnetic spin susceptibility below the structural transition is consistent with this concept. On the other hand, an itinerant scenario was put forward in Ref. [7]. These authors suggested that the driving force of dimerization is covalent bonding.

In order to analyze these scenarios we performed full structural relaxations of Li_2RuO_3 within DFT as implemented in the VASP code [22]. The final energies were computed using the all-electron method FPLO [23]. We considered a large sampling of initial structures, including the experimentally reported structures, and found several energetically favorable structures; the simplest two are shown in Figs. 4(a) and 4(b). The main results of our calculations are as follows: (1) The calculated ground state corresponds to a strong bond disproportionation ($l_l/l_s \sim 1.2$), in quantitative agreement with the experiment. (2) The disproportionation was only slightly modified when magnetization of Ru is included. (3) Examination of the electronic structure calculations shows that for each bond there is one pair of Ru $4d$ orbitals that can overlap directly via σ bonding (in an appropriately chosen local coordinate system, these could be selected as xy orbitals), with the amplitude $t_{dd\sigma}$, and two that can overlap indirectly through two bridging oxygens with the amplitude $\pm t_{pd\pi}^2/(E_d - E_p)$ (see Refs. [19,20,21] for details). One can also construct linear combinations, $u_+ = (xz + yz)/\sqrt{2}$ and $u_- = (xz - yz)/\sqrt{2}$. Both of them provide the same hoppings via bridging oxygens, but only the former gives a direct hopping ($t_{dd\pi}$) of π nature. For really short dimers (the low-T phase) the direct hopping dominates, although it is largely offset by the indirect hopping, and as a result the bonding-antibonding splitting between the u_+ orbitals is larger than between u_-, but both are much smaller than the splitting due to the xy orbitals. This behavior is illustrated in the DOS shown in Figs. 4(c) and 4(d), where the directly overlapping xy orbitals form a very strong covalent bond (bonding-antibonding splitting of more than 2 eV). One of the two holes of Ru residing in the t_{2g} band is occupying this *anti*bonding state, with a substantial energy gain.

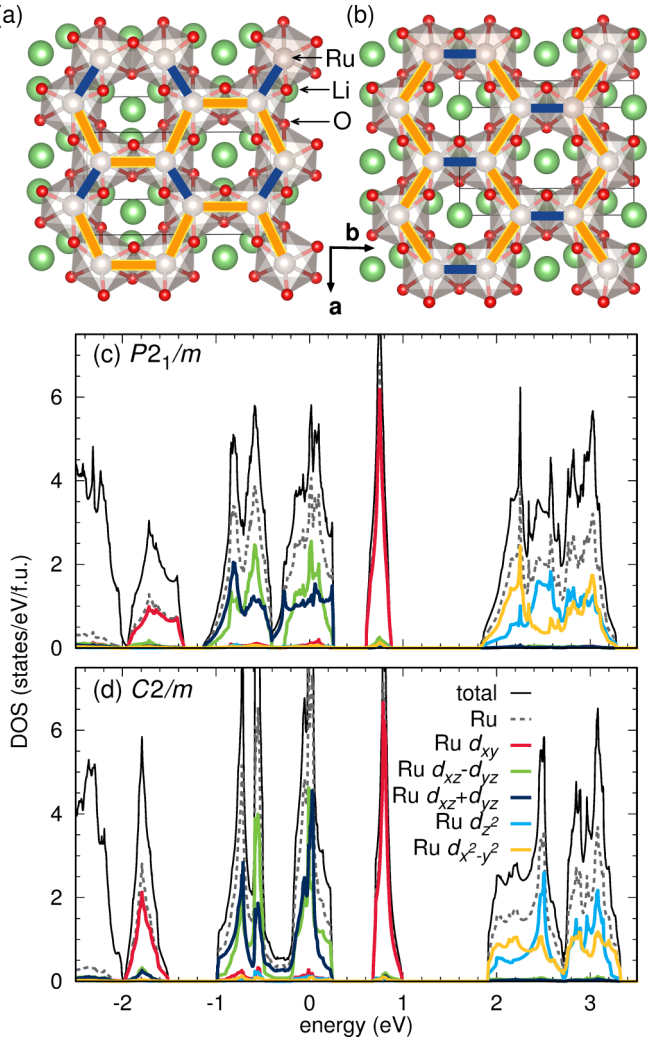

FIG. 4. (Color online) Armchair (a) and parallel (b) dimerized structures of Li_2RuO_3 investigated in this work. Shorter (dimerized) Ru-Ru bonds are marked with a dark bar, longer bonds with a light bar. The Ru DOS for these two low-energy structures are shown in panels (c) and (d), respectively.

(4) The u_- orbital also contributes to the total covalency, albeit considerably less. The corresponding bonding-antibonding splitting is about 0.7 eV and the second hole takes advantage of this fact. Moreover, this contribution is only weakly dependent on the bond length, and therefore its contribution to dimerization is much smaller than to covalency in general. (5) Examination of the Ru effective moment in spin-polarized calculation shows that it is at most spin 1/2 and never 1; this indicates that at least one electron spin is quenched. The second, $u_\pm$, spin may or may not be quenched depending on temperature. Our calculations find rather small energy differences between ferro- and antiferromagnetic arrangement of the $u_\pm$ spins, so when they are unbound and their covalent bond is broken at high temperature, they behave magnetically as nearly free spin 1/2 electrons. Indeed the difference between the experimental susceptibility at low temperatures (spin gap) and at high temperatures [7] is consistent with this scenario. (6) Finally, all investigated long-range orders of the structural dimers are energetically favorable when compared with the undimerized structure. The differences among the dimerized structures are of the order of 40 meV, comparable with the ordering transition temperature. On the other hand, the (optimized) uniform structure is 155 meV above the ground state structure, which explains why dimers themselves survive well above T_c.

Discussion. Our experimental results combined with theoretical calculations render the following picture: Ru-Ru bonds in Li_2RuO_3 have a very strong tendency to form local dimers with covalent bonds via direct overlap of Ru 4*d* orbitals [13]. The structural transition at ∼270 °C is of the order-disorder type: the dimers at $T \lesssim 270$ °C do not disappear at higher temperatures, nor does their concentration (1/3 of all bonds) change. Dimer-dimer interaction, presumably of elastic origin [as evidenced by the fact that the disordered phase has a larger *a* lattice parameter (see SM), due to a lack of proper dimer packing], is much weaker and responsible for mutual ordering of the dimers in the observed "armchair" structure. [18] In the high-temperature phase there is no ordering of dimers at a length scale $\gtrsim$1.5 nm, or 2–3 lattice parameters. The ordering temperature is consistent with the calculated energy differences between dimerized phases with different dimer long-range ordering. Upon quick cooling to 50°, the long-range dimer ordering was restored suggesting that the high-temperature phase is a valence bond liquid, where dimerization occurs dynamically on a time scale long compared to the characteristic time scale of our x ray measurements. While the concept of quantum spin liquid of dynamically disordered spin singlets is well known, its classical analog, a liquid of valence bonds dynamically disordered due to thermal fluctuations, as it is our case, has been less investigated [24]. Statistical physics of such an object should be nontrivial, bearing resemblance to Maier-Saupe transitions in liquid crystals and solid hydrogen [25]. Such a local dimer scenario may be also realized in the $4d^5$ and $5d^5$ counterpart systems. We hope that our results will stimulate further experimental and theoretical studies in this direction.

We thank M. Di Michiel and G. Khalliulin for useful discussions and the ESRF for support. I.I.M. acknowledges support from the Office of Naval Research (ONR) through the Naval Research Laboratory's Basic Research Program. M.A., H.O.J., and R.V. thank the German Science Foundation (DFG) for funding through SFB/TRR 49 and FOR 1346. S.S.V. thanks the Russian Foundation for Basic Research and the Ministry of Education and Science of Russia for Research Programs No. RFFI-13-02-00374 and No. MK-3443.2013.2. The work of D.Kh. was supported by the DFG via FOR 1346 and Research Grant No. 1484/2-1, and by Cologne University via the German excellence initiative.

[1] A. Shitade, H. Katsura, J. Kuneš, X.-L. Qi, S.-C. Zhang, and N. Nagaosa, Phys. Rev. Lett. **102**, 256403 (2009).

[2] G. Jackeli and G. Khaliullin, Phys. Rev. Lett. **102**, 017205 (2009).

[3] S. K. Choi, R. Coldea, A. N. Kolmogorov, T. Lancaster, I. I. Mazin, S. J. Blundell, P. G. Radaelli, Y. Singh, P. Gegenwart, K. R. Choi, S. W. Cheong, P. J. Baker, C. Stock, and J. Taylor, Phys. Rev. Lett. **108**, 127204 (2012).

[4] I. I. Mazin, S. Manni, K. Foyevtsova, H. O. Jeschke, P. Gegenwart, and R. Valentí, Phys. Rev. B **88**, 035115 (2013).

[5] Y. Miura, Y. Yasui, M. Sato, N. Igawa, and K. Kakurai, J. Phys. Soc. Jpn. **76**, 033705 (2007).

[6] H. Gretarsson, J. P. Clancy, Y. Singh, P. Gegenwart, J. P. Hill, J. Kim, M. H. Upton, A. H. Said, D. Casa, T. Gog, and Y-J. Kim, Phys. Rev. B **87**, 220407 (2013).

[7] Y. Miura, M. Sato, Y. Yamakawa, T. Habaguchi, and Y. Ono, J. Phys. Soc. Jpn. **78**, 094706 (2009).

[8] P. W. Anderson, Science **235**, 1196 (1987).

[9] D. S. Rokhsar, and S. A. Kivelson, Phys. Rev. Lett. **61**, 2376 (1988).

[10] S. A. J. Kimber, C. D. Ling, D. J. P. Morris, A. Chemseddine, P. F. Henry, and D. N. Argyriou, J. Mater. Chem. **20**, 8021 (2010).

[11] See Supplemental Material at http://link.aps.org/supplemental/10.1103/PhysRevB.89.081408 for details of theoretical and experimental methods as well as tabulated crystal structures.

[12] A. Larson and R. V. Dreele, General Structure Analysis System (GSAS), Los Alamos National Laboratory Report LAUR 86–748, 1994.

[13] Note that the measured short bond is shorter than the Ru-Ru metallic bond distance of 2.65 Å.

[14] The population of the three distances is extracted from the intensity of the peaks (Fig. 2). If there were a significant change in the population of the various types of bonds, then a strong misfit would be observed in the difference profile [Fig. 2(a)].

[15] C. L. Farrow, P. Juhas, J. W. Liu, D. Bryndin, E. S. Božin, J. Bloch, Th. Proffen, and S. J. L. Billinge, J. Phys.: Condens. Matter **19**, 335219 (2007).

[16] S. A. J. Kimber, M. S. Senn, S. Fratini, H. Wu, A. H. Hill, P. Manuel, J. P. Attfield, D. N. Argyriou, and P. F. Henry, Phys. Rev. Lett. **108**, 217205 (2012).

[17] The idea is to fit the same model over different r ranges of the PDF data. We used an 8.5 Å box and stepped r-min from 1.5 to 32.5 Å in 2.5 Å steps.

[18] G. Jackeli and D. I. Khomskii, Phys. Rev. Lett. **100**, 147203 (2008).

[19] $t_{pd\pi}$ corresponds to the Ru d–O p hopping amplitude of π nature and $E_d - E_p$ is the energy difference between Ru d and O p states.

[20] I. I. Mazin, H. O. Jeschke, K. Foyevtsova, R. Valentí, and D. I. Khomskii, Phys. Rev. Lett. **109**, 197201 (2012).

[21] K. Foyevtsova, H. O. Jeschke, I. I. Mazin, D. I. Khomskii, and R. Valentí, Phys. Rev. B **88**, 035107 (2013).

[22] G. Kresse and J. Hafner, Phys. Rev. B **47**, 558 (1993).

[23] K. Koepernik and H. Eschrig, Phys. Rev. B **59**, 1743 (1999); http://www.FPLO.de.

[24] S. Lakkis, C. Schlenker, B. K. Chakraverty, R. Buder, and M. Marezio, Phys. Rev. B **14**, 1429 (1976).

[25] A. F. Goncharov, I. I. Mazin, J. H. Eggert, R. J. Hemley, and H.-k. Mao, Phys. Rev. Lett. **75**, 2514 (1995).